A molecular dynamics model of the atomic structure of Tb metaphosphate glass $(Tb_2O_3)_{0.25}(P_2O_5)_{0.75}$

2006 J. Phys.: Condens. Matter 18 6815

(http://iopscience.iop.org/0953-8984/18/29/019)

INSTITUTE OF PHYSICS PUBLISHING JOURNAL OF PHYSICS: CONDENSED MATTER

J. Phys.: Condens. Matter **18** (2006) 6815–6826 doi:10.1088/0953-8984/18/29/019

A molecular dynamics model of the atomic structure of Tb metaphosphate glass $(Tb_2O_3)_{0.25}(P_2O_5)_{0.75}$

E B Clark, R N Mead and G Mountjoy[1]

School of Physical Sciences, University of Kent, Canterbury CT2 7NH, UK

E-mail: g.mountjoy@kent.ac.uk and mountjoy@unica.it

Received 24 April 2006, in final form 12 June 2006
Published 6 July 2006
Online at stacks.iop.org/JPhysCM/18/6815

Abstract

There have been many recent experimental studies of rare earth (RE) phosphate glasses, $(RE_2O_3)_x(P_2O_5)_{1-x}$, but only two previous reverse Monte Carlo (RMC) modelling studies. The current study reports the first molecular dynamics model of an RE phosphate glass, for Tb metaphosphate glass, with $x = 0.25$. The model is in good agreement with experimental results for nearest-neighbour distances and coordination numbers, and in reasonable agreement for x-ray and neutron diffraction structure factors. There is a tetrahedral phosphate network, with marked splitting of distances from P to bridging oxygen (O_b) and from P to non-bridging oxygen (O_{nb}). The phosphate network has tetrahedra denoted Q^n (where n is the number of O_b) with an average of $n = 2.1$ and mostly Q^2 groups, but with some Q^1 and Q^3 groups. Most Tb are coordinated to six O_{nb}, and the average coordination is $N_{TbO_{nb}} = 5.7$, which compares favourably with experimental results that indicate $N_{RE-O} \sim 6$ in metaphosphate glasses with small RE ions. The great majority of O_{nb} are bonded to only one Tb, but there are a few shared O_{nb} occurring in Tb–O_{nb}–Tb configurations. These cause a small peak in Tb–Tb correlations around 4 Å, prior to the main peak around 6 Å. The corresponding Tb–Tb partial structure factor shows promising agreement with a recent experimental measurement using magnetic neutron scattering.

1. Introduction

Rare earth elements (RE) can be difficult to incorporate into oxide glasses in large amounts (i.e. larger than for RE-doped glasses) [1]. However, with melt quenching it is possible to obtain RE phosphate glasses, $(RE_2O_3)_x(P_2O_5)_{1-x}$, with large RE contents of up to $x = 0.25$, i.e. the metaphosphate composition. The incorporation of RE into phosphate glasses gives

[1] Author to whom any correspondence should be addressed. Present address: Dipartimento di Scienze Chimiche, Università di Cagliari, Complesso Universitario, SS 554 bivio per Sestu, 09042 Monserrato, Cagliari, Italy.

these glasses interesting optical and magnetic properties due to the RE 4f electrons. The potential applications stemming from these properties, e.g. lasers and Faraday rotators [2], have motivated many structural studies of RE phosphate glasses in recent years. These structural studies also provide a test for principles of glass structure.

Metal phosphate glasses are known to contain a network of PO_4 tetrahedra, and this has been shown for RE phosphate glasses by diffraction results for P–O correlations [3]. In PO_4 tetrahedra, there are P bonds to bridging oxygen, O_b, and to non-bridging oxygen, O_{nb}, and these have different bond valence. P–O_{nb} bonds are shorter than P–O_b bonds, and neutron diffraction studies have shown the difference to be 0.12(2) Å [3]. The P–O_{nb} bond valence also depends on the number of O_b in the tetrahedra, which is equal to the connectivity n of a PO_4 group, denoted Q^n. Infrared (IR) and Raman spectroscopy are sensitive to different Q^n groups and, as expected, results for RE metaphosphate glasses show a dominance of Q^2 groups [4, 5]. However, results for glasses with $x \approx 0.25$ and RE = Sm [4] and Gd [5] also show some intensity around 1350 cm^{-1}, which is characteristic of isolated Q^3 groups in a Q^2 network [6]. ^{31}P nuclear magnetic resonance (NMR) spectra of RE phosphate glasses show broad peaks which are difficult to resolve among $Q^1/Q^2/Q^3$ groups [7]. Results for a glass with RE = Nd and $x = 0.18$ indicated a majority of Q^2 with some Q^3, as expected [8]. Results for a glass with RE = La and $x = 0.23$ indicated a majority of Q^2, but the expected small contribution from Q^3 could not be distinguished [7].

Much interest in RE phosphate glasses has focussed on RE coordination number N_{RE-O}, and how this depends on RE ion size (related to the lanthanide contraction) and concentration (related to conceptual models discussed below). Note that Al and Si impurities have been found in RE phosphate glasses, due to contamination from crucibles [9–12] (and these are indicated below). Newport and co-workers used x-ray [8] and neutron diffraction [9], and L_3-edge [13] and K-edge [14] EXAFS for glasses with a range of RE from La to Er and x from 0.18 to 0.26 (Al impurities reported). They found $N_{RE-O} \approx 6.0(5)$ for small RE ions (beyond Gd) and ≈7.0(5) for large RE ions (up to Nd), with Sm/Eu/Gd being intermediate. Hoppe and co-workers used x-ray and neutron diffraction and for glasses with RE = La [10, 15] and Nd [16] (with silica crucibles used). They found $N_{RE-O} \approx 7.1(5)$ for $x = 0.25$ and 6.8(3) for $x = 0.20$ in $(La_2O_3)_x(P_2O_5)_{1-x}$ glasses [10, 15], and 6.6(3) for $x = 0.25$ and 6.9(3) for $x = 0.20$ in $(Nd_2O_3)_x(P_2O_5)_{1-x}$ glasses [16]. In a later study [17] for $x \approx 0.25$ (with Si impurities reported), they found $N_{RE-O} \approx 6.3(3)$ for small RE ions (beyond Gd) and ≈6.8(3) for large RE ions (up to Gd). For $x \approx 0.13$ they found $N_{RE-O} = 8.5(3)$ for large RE ions (up to Nd). Brow and co-workers used L_3-edge EXAFS for glasses with RE = Nd and Er [18] (with Si impurities reported). For RE = Nd they found $N_{RE-O} = 6.4(9)$ and 9(1) for $x = 0.25$ and 0.15 respectively. For RE = Er they found $N_{RE-O} = 6.3(6)$ and 7.3(4) for $x = 0.28$ and 0.18, respectively. Salmon and co-workers used neutron diffraction with isomorphic substitution for glasses with $x \approx 0.22$ (with Al impurities reported) and they found $N_{RE-O} = 7.5(2)$ and 6.7(1) for RE = La/Ce [11] and Dy/Ho [12], respectively.

The previous structural studies of RE phosphate glasses have been accompanied by the development of conceptual models. The examination of oxide crystal structures shows that RE can be found with a wide range of N_{RE-O} values from 6 to 12. In RE metaphosphate crystals, $N_{RE-O} = 8$ for large RE ions [19] (with six shorter and two longer bonds), and 6 for small RE ions [20], with Sm/Eu/Gd falling in both groups. RE ultraphosphate crystals [19] have $x = 0.167$ and $N_{RE-O} = 8$ (with eight equal bonds). For metal phosphate glasses, Hoppe proposed that metal cations maximize their coordination for the number of O_{nb} available [10, 21]. The latter is equal to $(2x + 1)/x$ per RE, which gives $N_{RE-O} = 6$ for $x = 0.25$ (metaphosphate) and 8 for $x = 0.167$ (ultraphosphate). To obtain $N_{RE-O} > 6$ for $x = 0.25$, it is necessary to include the effect of O_{nb} shared between RE. As discussed by

Salmon and co-workers [11, 12], $N_{RE-O} = 7$ requires 1/6 of O_{nb} (or 1/7 of O_{nb} neighbours) to be shared, and $N_{RE-O} = 8$ requires 1/3 of O_{nb} (or 1/4 of O_{nb} neighbours) to be shared. Sharing of O_{nb} between RE creates RE–O_{nb}–RE configurations, and consequently short RE–O_{nb}–RE distances, with $R_{RE-RE} < 2R_{RE-O}$ (as seen in metaphosphate crystals with large RE ions).

Modelling studies of glass structure can confirm the interpretation of experimental results, can demonstrate that a consistent three-dimensional structure exists, and can reveal structural features that are difficult to observe experimentally (e.g. RE–RE correlations). Previous modelling studies of (non-RE) metal phosphate glasses have used molecular dynamics (MD) and, more commonly, reverse Monte Carlo (RMC) dynamics. RMC gives excellent agreement with diffraction data, but does not always produce smooth short-range order (i.e. nearest-neighbour peaks), whereas the contrary can be said of MD. This follows from the different constraints used in these two types of modelling. MD modelling of phosphate glasses has previously been reported for Li [22], Na [23], Mg, Zn and Pb [24] metaphosphate glasses. There have only been two previous RMC modelling studies of RE phosphate glass. Hoppe and co-workers used RMC to obtain a model for RE = La with $x = 0.25$ [15]. The model was consistent with x-ray and neutron diffraction data, and had average $N_{RE-O} = 6.5$, but also contained some three coordinated P and some RE bonds to O_b, both of which are unlikely to be present in the experimental glass. Newport and co-workers used RMC to obtain models for glasses with RE = Eu and Tb and $x \approx 0.25$ [25]. The models were consistent with x-ray diffraction data, and had 98% PO_4 tetrahedra in Q^2 groups, and 95% of RE with $N_{RE-O} = 6$ (bonded only to O_{nb}).

The current study presents the first MD model of an RE phosphate glass, in this case Tb metaphosphate glass. Tb comes at the beginning of the second half of the lanthanide series, and Tb^{3+} is representative of small RE ions (in the context of the above discussion of experimental results), with an ion size of 1.00 Å compared to 1.15 Å for La^{3+} and 0.93 Å for Lu^{3+}. Tb metaphosphate glass is of particular interest due to the recent experimental measurement of Tb–Tb correlations [26].

2. Molecular dynamics method

P–O, Tb–O and O–O interactions were described using rigid ion potentials, as this allows a large number of time-steps (important for modelling glasses). The parameters were taken from those derived by Teter [27], and were evaluated to establish their suitability (discussed below). Although these have not previously been used to model phosphate glasses, other potential parameters from Teter have proven effective for modelling silicate [28] and aluminate [29] glasses. The potentials have the form

$$V_{ij}(r) = \frac{q_i q_j}{4\pi\varepsilon_0 r} + A_{ij}\exp\left(\frac{-r}{\rho_{ij}}\right) - \frac{C_{ij}}{r^6} \tag{1}$$

where $V_{ij}(r)$ is the potential, i and j are element types, r is interatomic distance, q is charge, and A_{ij}, ρ_{ij} and C_{ij} are potential parameters (with $\varepsilon_0 = 8.854 \times 10^{-12}$ C^2 N^{-1} m^{-2}). The potential parameters are shown in table 1. In addition, potential parameters for O–P–O and P–O–P bond bending interactions were taken from [22], and have the form

$$V_{jji}(\theta) = \tfrac{1}{2}k_{jji}(\theta - \Theta_{jji})^2 \tag{2}$$

where j is the element type of the central atom, $k_{jji} = 3.5$ eV and $\Theta_{jji} = 109.47°$ for O–P–O, and $k_{jji} = 3.0$ eV and $\Theta_{jji} = 135.5°$ for P–O–P. The potential parameters were evaluated by using the GULP program [30] to model crystals of P_4O_{10} (a molecule), o-P_2O_5, o′-P_2O_5, Tb_2O_3 (types B and C), $TbPO_4$ (orthophosphate), TbP_3O_9 (metaphosphate), and

Table 1. Potential parameters for two-body interactions used in the current study, which were taken from those derived by Teter [27]. (Potential parameters for three-body interactions were taken from [22] and are detailed in the text.)

ij	q_i (e)	A_{ij} (eV)	ρ_{ij} (Å)	C_{ij} (eV Å^{-6})
PO	3.0	27 722	0.1819	86.86
TbO	1.8	13 137	0.2287	36.33
OO	−1.2	1 844	0.3436	192.58

Table 2. Structural parameters for Tb_2O_3–P_2O_5 crystals from the CDS database [31] (non-italic) and from energy minimization for potential parameters used in the current study (italic). (P_4O_{10} was modelled as a single, isolated molecule in a large unit cell. Monoclinic YbP_3O_9 crystal* was used as the estimated starting structure for monoclinic TbP_3O_9 crystal.)

Average	P_4O_{10}	o-P_2O_5	o′-P_2O_5	Tb_2O_3 type B	Tb_2O_3 type C	$TbPO_4$	YbP_3O_9* *TbP*$_3$*O*$_9$	TbP_5O_{14}
a (Å)	—	16.314	9.193	14.030	10.729	6.931	11.219*	8.721
		16.502	*8.623*	*14.285*	*10.640*	*6.763*	*11.052*	*8.655*
b (Å)	—	8.115	4.890	3.536	10.729	6.931	19.983*	8.877
		8.072	*5.073*	*3.427*	*10.640*	*6.763*	*19.854*	*8.868*
c (Å)	—	5.265	7.162	8.717	10.729	6.061	9.999*	12.910
		4.768	*6.921*	*8.668*	*10.640*	*6.344*	*9.970*	*13.098*
Vol (Å^3)	—	697	321	425	1235	291	2223*	999
		635	*302*	*418*	*1204*	*290*	*2171*	*984*
N_{PO}	4	4	4	—	—	4	4*	4
	4	*4*	*4*			*4*	*4*	*4*
R_{PO} (Å)	1.55	1.54	1.54	—	—	1.54	1.54*	1.54
	1.52	*1.51*	*1.51*			*1.50*	*1.50*	*1.50*
O–P–O (deg)	109	109	109	—		109	109*	109
	109	*109*	*109*			*109*	*109*	*109*
P–O–P (deg)	122	131	142	—	—	—	137*	135
	132	*146*	*149*			—	*147*	*141*
N_{TbO}	—	—	—	6.67	6	8	6*	8
				6.67	*6*	*8*	*6*	*8*
R_{TbO} (Å)	—	—	—	2.39	2.31	2.37	2.21*	2.43
				2.37	*2.29*	*2.42*	*2.27*	*2.47*

TbP_5O_{14} (ultraphosphate). The crystal structures were obtained from the CDS database [31] (the monoclinic YbP_3O_9 crystal was used as a starting structure for the monoclinic TbP_3O_9 crystal, since the CDS database [31] contains the former but not the latter). The results are shown in table 2. Although there is a tendency for R_{PO} to be slightly too short and the P–O–P bond angle to be slightly too large, the results are quite reasonable, given that eight structures are modelled with 14 potential parameters.

MD modelling was used to obtain a model of atomic structure of $(Tb_2O_3)_x(P_2O_5)_{1-x}$ glass with composition $x = 0.25$. The impurity-free system was chosen as a more robust starting point for modelling, since modelling the effect of an impurity would be more challenging (as there are fewer atoms in the model, and less experimental data, for the impurities). Although the experimental glass has Al impurities [8, 9, 13, 26], the ratio of Al:Tb is ∼1:8 [26], so Al can be expected to have a perturbing but not dominant effect on Tb coordination. The model has a total of 1300 atoms (100 Tb, 300 P and 900 O) in a cubic box with a length of 26.5 Å. A random starting configuration and periodic boundary conditions were used. One objective of the modelling work was to produce a model which agreed with the experimental density of

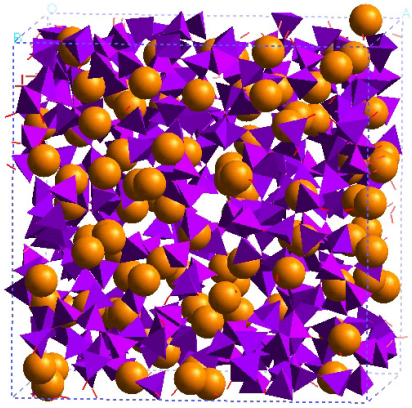

Figure 1. Image of the model of Tb metaphosphate glass (tetrahedra show the phosphate network, and spheres show Tb^{3+} ions).

(This figure is in colour only in the electronic version)

3.58 g cm^{-3} [8], as this is one of the requirements for a model to represent an experimental glass. However, use of an NPT algorithm with $P = 1$ atm produced a model with a density 8% higher than experiment. Hence an NVT algorithm was used to obtain a model matching the experimental density. As a consequence, the model obtained has an unphysical negative pressure. This means a greater volume for the structural configuration, but does not noticeably increase values of R and N, because the latter are dominated by the short-range part of the potentials. (It is often difficult to model both the density and pressure of glasses accurately using MD, e.g. in [32].)

MD modelling used the DLPOLY program [33], with time-steps of 1 fs. A Berensden NVT algorithm was used with a relaxation time of 2 ps. A short-range cut-off of 10 Å was used for all except the Coulomb potential, and the Coulomb potential was calculated using the Ewald method with a precision of 10^{-5}. The modelling used six stages. The first three stages were temperature baths of 80 000 time-steps (with equilibration) at 6000, 3000, and 1500 K, and with linear thermal expansion coefficients of 1.03, 1.015, and 1.005, respectively. (A trajectory of 80 000 time-steps at 6000 K is sufficient to allow diffusion over the box length.) This was followed by a temperature quench of 60 000 time-steps (with equilibration) from 1500 to 300 K, i.e. a quench rate of 10^{13} K s^{-1}. This quench rate is typical in MD studies of glasses, e.g. in [22, 28, 32]. Due to constraints on computing time, all MD studies of glasses use quench rates that are several orders of magnitude higher than in experiments. Despite this (the role of quench rates is under ongoing investigation, e.g. in [34]), MD studies have been able to provide key insights into glass structures. The final two stages were temperature baths of 80 000 time-steps at 300 K (the first with equilibration and the second without equilibration). During the final stage, structural parameters were sampled (every 200 time-steps) to include disorder due to thermal vibrations, which is present in the experimental results.

3. Results

Figure 1 shows an image of the model of Tb metaphosphate glass, and the tetrahedral PO_4 network is evident. Figure 2 shows the partial radial distribution functions $T_{ij}(r)$ for the model,

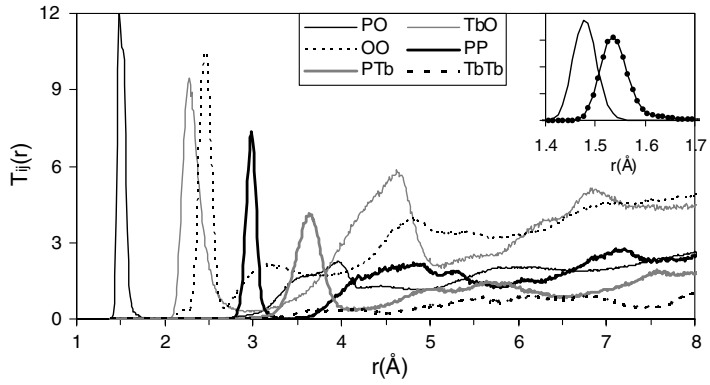

Figure 2. Partial radial distribution functions $T_{ij}(r)$ for a model of Tb metaphosphate glass. The inset shows P–O_b (dotted) and P–O_{nb} (solid) correlations. (Note that P–O, P–P, P–Tb and Tb–Tb correlations have been scaled ×0.5, ×1.5, ×3, and ×1.5, respectively.)

where i and j are element types. $T_{ij}(r)$ are defined as

$$T_{ij}(r) = \frac{1}{r}\left(\frac{1}{N_i}\sum_{\ell=1}^{N_i}\sum_{m\neq\ell}^{N_j}\delta(r - R_{\ell m})\right) = 4\pi r\rho_j g_{ij}(r) \tag{3}$$

where $g_{ij}(r)$ is the partial pair distribution function with $g_{ij}(r) \to 1$ as $r \to \infty$, and ρ_j is the atomic number density of element type j ($\ell = 1 - N_i$ is the index over atoms of element type i). The first peak in $T_{PO}(r)$ at ∼1.5 Å represents P–O nearest neighbours. All oxygen atoms have either two bonds to P (34.5% of oxygen, denoted O_b) or one bond to P (65.5% of oxygen, denoted O_{nb}). The inset of figure 2 shows that P–O_{nb} bonds are shorter than P–O_b bonds, as expected. In the model, these bonds differ by 0.06(1) Å, whereas differences of 0.11(1) Å have been reported in neutron diffraction results for glasses with $x = 0.25$ and RE = La [15] and Nd [16]. The model has 96.4% P with four-fold coordination. The remaining 3.6% of P have five-fold coordination, and this should be considered as a defect arising from slight inaccuracy in the potentials. $T_{OO}(r)$ has a first peak at ∼2.5 Å due to O–P–O configurations (a very small feature at 2.2 Å occurs due to five-fold coordinated P defects). Figure 3 shows that the average O–P–O bond angle is tetrahedral, i.e. 109° (a very small feature at 85° occurs due to five-fold coordinated P defects). The inset of figure 3 shows that O_{nb}–P–O_{nb} bond angles are expanded, and O_b–P–O_b bond angles are contracted. This is expected, since O_{nb}–O_{nb} neighbours experience greater repulsion than O_b–O_b neighbours.

$T_{PP}(r)$ has a narrow first peak at ∼3.0 Å representing P–P nearest neighbours in the phosphate network, and figure 3 shows that P–O–P bond angles are peaked at around 150°. The connectivity of the phosphate network can be described by the Q^n distribution (each P is classified as Q^n, where $n = N_{PO_b}$), and there is a majority of Q^2 groups (50.3%) but also significant amounts of Q^1 (24.0%) and Q^3 (21.0%) groups, with an average of $n = 2.1$ (the tiny remainder of Q^n groups are Q^0 and Q^4). This average n is slightly high (due to five-fold coordinated P defects) compared to the expected average of $n = 2.0$ for the metaphosphate composition. Another way to describe the topology of a tetrahedral network is by the distribution of rings (formed by connected tetrahedra), as discussed for silicate glasses in [35]. The model has only a few rings with sizes from 4 to 14, averaging 0.03 rings per P (the distribution of ring sizes was calculated using the method of shortest path analysis, and the statistics for ring sizes larger than 14 are not considered, as they can be affected by the finite box size). This is expected for a majority of Q^2 units forming long chains, and is similar to the

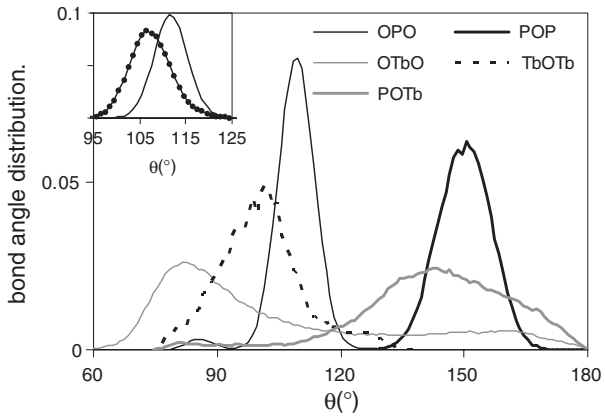

Figure 3. Bond angle distributions for a model of Tb metaphosphate glass. The inset shows O_b–P–O_b (dotted) and O_{nb}–P–O_{nb} (solid) bond angle distributions. (Note that O_b–P–O_{nb} bond angles are omitted for clarity.)

Table 3. Nearest-neighbour distances R_{ij}, and coordination numbers N_{ij}, of $(Tb_2O_3)_x(P_2O_5)_{1-x}$ glass for experiments with $x = 0.26$, and for the model with $x = 0.25$. (The splitting of P–O_{nb}/P–O_b distances is shown for neutron diffraction and MD results.)

	X-ray diffr. [8]	Neutron diffr. [9]	EXAFS [13]	MD
R_{PO} (Å)	1.56(1)	1.49(1)/1.60(1)	—	1.48/1.54
N_{PO}	3.8(3)	1.7(4)/1.9(4)	—	2.10/1.95
R_{TbO} (Å)	2.32(2)	2.27(2)	2.27(1)	2.28
N_{TbO}	6.6(6)	5.6(6)	5.8(2)	5.7
R_{OO} (Å)	2.58(3)	2.50(1)	—	2.46
N_{OO}	4.8(8)	3.4(3)	—	4.1
R_{PP} (Å)	2.96(4)	3.00(4)	—	2.99
N_{PP}	4.1(13)	2.0(9)	—	2.1

distribution of rings sizes reported for $CaSiO_3$ [36] and Na_2SiO_3 [35] glasses (which also have an average of $n = 2.0$).

The first peak in $T_{TbO}(r)$ at ∼2.3 Å represents Tb–O nearest neighbours. The majority of Tb (62%) has six-fold coordination, with nearly all of the remaining Tb (34%) having five-fold coordination, giving an average $N_{TbO} = 5.7$. All Tb is bonded only to O_{nb}. $T_{OO}(r)$ has a broad second peak from 3.0 to 3.5 Å representing O_{nb} coordinated to Tb, i.e. O_{nb}–Tb–O_{nb} configurations. The O_{nb}–Tb–O_{nb} bond angle shown in figure 3 represents TbO_N polyhedra, and is peaked at ∼80° with a shoulder at larger angles extending to 180°, as expected for distorted octahedral coordination. P–Tb correlations are first prominent from 3 to 4 Å, and the Tb–Tb correlations show a small peak around 4 Å followed by a larger, broad peak around 6 Å. The former arises due to sharing of O_{nb}, i.e. Tb–O_{nb}–Tb configurations, or corner-sharing TbO_N polyhedra.

Experimental results have been reported only for one Tb glass, with a composition of $(Tb_2O_3)_x(Al_2O_3)_y(P_2O_5)_{1-x}$, with $x = 0.25$ [8, 9, 13, 26] and $y = 0.03$ (i.e. Al impurity due to the use of an alumina crucible) [28], which is close to the metaphosphate composition. The experimental results for nearest-neighbour distances R_{ij} and coordination numbers N_{ij} are reported in table 3 for P–O, Tb–O, O–O and P–P correlations. There is good agreement with the modelling results, considering the reported experimental uncertainties. The x-ray results for

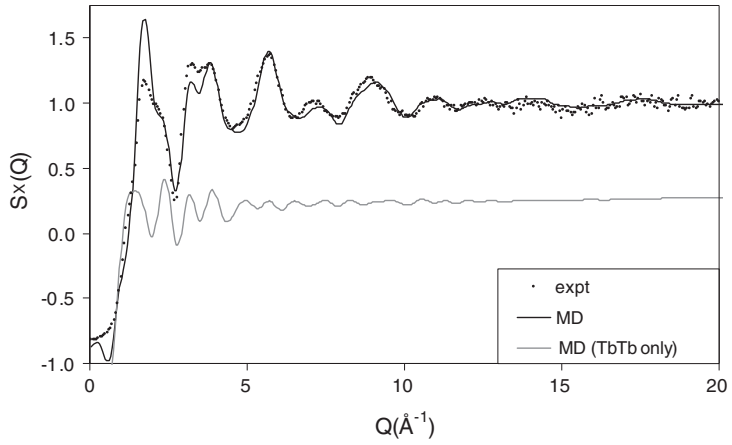

Figure 4. X-ray diffraction structure factor $S_X(Q)$ of $(Tb_2O_3)_x(P_2O_5)_{1-x}$ glass for the model with $x = 0.25$ (solid), and from experiment with $x = 0.26$ (dotted) [8]. (The contribution of only Tb–Tb correlations (grey) is $w_{TbTb}(Q)S_{TbTb}(Q)$.)

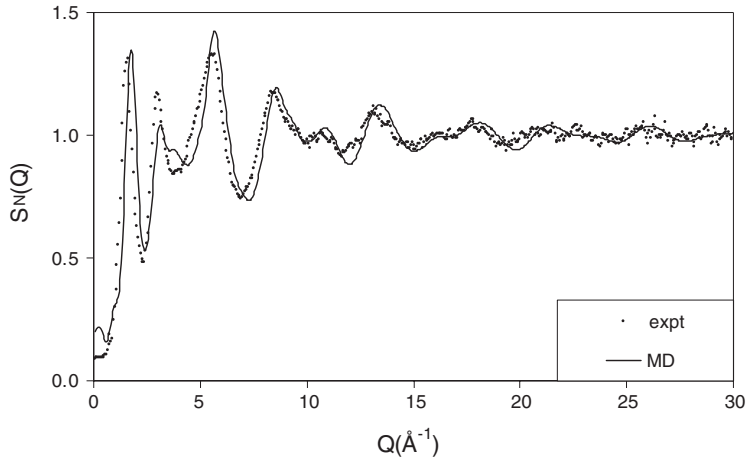

Figure 5. Neutron diffraction structure factor $S_N(Q)$ of $(Tb_2O_3)_x(P_2O_5)_{1-x}$ glass for the model with $x = 0.25$ (solid), and from experiment with $x = 0.26$ (dotted) [9].

O–O correlations, and the neutron results for P–P correlations, are somewhat uncertain due to the small weighting of the corresponding partials (see equation (4)). The model value of R_{PO_b} is ∼0.05 Å shorter than the neutron diffraction result of 1.60 Å [9] (neutron diffraction results for other RE metaphosphate glasses also give $R_{PO_b} = 1.60$ Å [15, 16]). The model has a value of $R_{OO} = 2.46$ Å, which is somewhat smaller than the x-ray diffraction result of 2.58(3) Å, but which shows less discrepancy with the neutron diffraction result of 2.50(1) Å. Figures 4 and 5 (respectively) show experimental x-ray [8] and neutron [9] diffraction structure factors $S(Q)$. The $S(Q)$ from the model have been calculated using

$$Q(S(Q) - 1) = \sum_{ij} w_{ij}(Q) \int (T_{ij}(r) - 4\pi r\rho_j) \sin(Qr)\, dr \tag{4}$$

where $w_{ij}(Q)$ is the weighting factor for scattering from correlations between elements i and j [37]. (The $S(Q)$ were calculated using $T_{ij}(r)$ up to $r = 10$ Å, for which case a cut-off

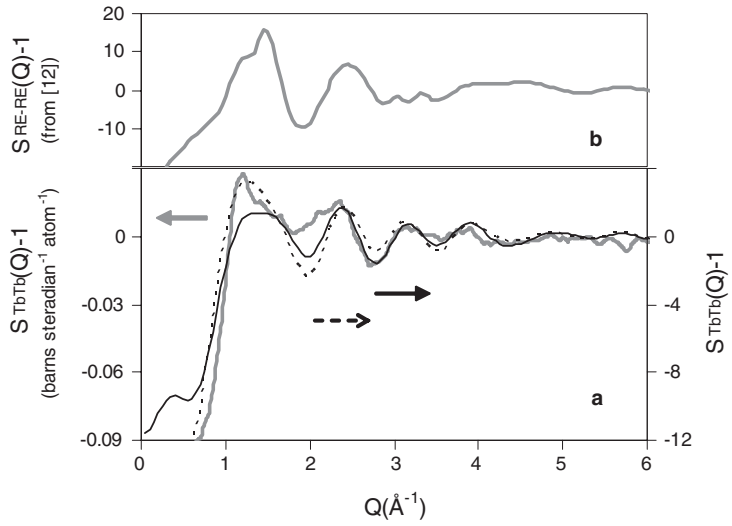

Figure 6. (a) Tb–Tb partial structure factor $S_{\mathrm{TbTb}}(Q)$ of $(Tb_2O_3)_x(P_2O_5)_{1-x}$ glass for the model with $x = 0.25$ (black) and from magnetic neutron scattering experiment with $x = 0.26$ (grey) [26]. Note that the experimental result has units of barns steradians^{-1} atoms^{-1} (left-hand y-axis) and hence is proportional to the model result (right-hand y-axis). (The dotted line shows $S_{\mathrm{TbTb}}(Q)$ for the model calculated after removing the small peak around 4 Å in $T_{\mathrm{TbTb}}(r)$.) (b) Experimental $S_{\mathrm{RE-RE}}(Q)$ reported in [12] for glasses with $x \approx 0.22$ and RE = Dy/Ho.

function is found to be unnecessary.) The model $S(Q)$, also shown in figures 4 and 5, are in reasonable agreement with the experimental $S(Q)$, although there is some mismatch in peak heights and positions. The oscillations in neutron diffraction $S(Q)$ are slightly out of phase, due to the slightly shorter value of $R_{\mathrm{PO_b}}$, as discussed above.

Newport *et al* recently carried out a magnetic neutron scattering study of Tb metaphosphate glass [26]. The neutron scattering length depends on the nuclear spin alignment, and a magnetic field can be used to align the nuclear spins of paramagnetic Tb^{3+} ions. Hence magnetic neutron scattering is one of the few experimental techniques which can directly probe Tb–Tb correlations. In this way it was possible to obtain a measurement of the Tb–Tb partial structure factor, $S_{\mathrm{TbTb}}(Q)$ (equation (4) with ij = Tb–Tb), the first time that such a measurement has been reported for a glass [26]. Figure 6(a) shows the model $S_{\mathrm{TbTb}}(Q)$ with the experimental results. The model result is in promising agreement, considering that a direct experimental measurement of RE–RE correlations necessarily involves a weaker signal.

4. Discussion

The current study presents the first MD model of an RE phosphate glass. This is a challenging modelling objective, due to the different characters of P–O and Tb–O interactions. The MD modelling used 14 potential parameters which reasonably accurately reproduced the known short-range order in eight Tb_2O_3–P_2O_5 crystal structures. The model of Tb metaphosphate glass contains a corner-shared tetrahedral PO_4 network, as expected. The short-range order in the phosphate network is in fairly good agreement with experimental results, with good values of R_{ij} and N_{ij} for P–O, O–O and P–P correlations. Some details are not completely satisfactory. There is a small content (3.6%) of five-fold coordinated P defects, and $R_{\mathrm{PO_b}}$ is $\sim$0.05 Å too short. Reducing these discrepancies would require the development of improved potentials, which is a complex task.

The connectivity of the phosphate network is also in fair agreement with the experimental results, with expected proportions of O_b and O_{nb}, and an average of $n = 2.1$, close to the expected value of $n = 2.0$. The Q^n distribution is peaked around Q^2, but includes significant amounts of Q^1 and Q^3. A broad distribution of Q^n is typically found in MD models of network glasses. However, ^{31}P NMR data for RE metaphosphate glasses does not establish the amounts of Q^1 and Q^3 present precisely. The model value of R_{PP} is similar to that from neutron diffraction. However, figure 3 shows that the P–O–P bond angle is peaked around 152°, and this is somewhat larger than experimental results, suggesting an angle of around 144° for a glass with RE = Tb and $x = 0.26$ [8, 9], and for other RE phosphate glasses [17] (an angle of 140° was reported for P_2O_5 glass [38]). Increasing the value of k_{POP} improves the value of the P–O–P bond angle, but causes poor results for Tb–O correlations.

As discussed in the introduction, overall experimental results for metaphosphate glasses with small RE ions (beyond Gd) indicate $N_{RE-O} \approx 6(0.5)$. The model has values of R_{TbO} and N_{TbO} in good agreement with experiment, and most Tb (62%) has coordination of 6. All Tb is bonded only to O_{nb}, as expected. At the metaphosphate composition there are 6 O_{nb} per Tb, hence a coordination of 6 is theoretically possible with no sharing of O_{nb} between Tb. Since O_{nb} are bonded to one P^{5+} ion and one RE^{3+} ion, it is less favourable for them to also be bonded to another RE^{3+} ion (although this does occur in RE metaphosphate crystals with large RE ions). The great majority of O_{nb} (78%) are bonded to just one Tb, and figure 3 shows that the typical P–O_{nb}–Tb bond angle is around 140°. However, there a few O_{nb} (14%) that are bonded to zero Tb, and a few O_{nb} (8%) that are bonded to two Tb. The latter involve Tb–O_{nb}–Tb configurations, which have Tb–O_{nb}–Tb bond angles around 100°. (Tb–O_{nb}–Tb bond angles are smaller than P–O_{nb}–Tb bond angles due to greater repulsion between cations in the latter.)

A conceptual model in which all Tb are six-fold coordinated and there is no sharing of O_{nb} implies there will be no short RE–O_{nb}–RE distances. Figure 1 shows that $T_{TbTb}(r)$ has a main peak around 6 Å, consistent with a great majority of unshared O_{nb}. Hoppe and co-workers have proposed [17] that, for La metaphosphate glass, the peak in La–La correlations at ∼6.4 Å corresponds to two La linked with two O_{nb} of the same Q^2 unit. Furthermore, they proposed that such La–La correlations give rise to features at low Q in the x-ray diffraction structure factor $S_X(Q)$, including a shoulder at $Q = 1.05$ Å^{-1}. According to their interpretation, the peak in Tb–Tb correlations at ∼6 Å could be expected to contribute to $S_X(Q)$ at $Q \approx 1.2$ Å^{-1} (the change in Q is inverse to the change in R_{RE-RE}, and the latter depends on the radius ratio of Tb^{3+}:La^{3+} which is 1.00 Å:1.15 Å). This appears consistent with the contribution of only Tb–Tb correlations to $S_X(Q)$ (i.e. $w_{TbTb}(Q)S_{TbTb}(Q)$), as shown in figure 4. (Note that figure 4 shows that Tb–Tb contributions contribute to $S_X(Q)$ over a range of Q values, including a shoulder at $Q \approx 1.2$ Å^{-1}.) Figure 2 shows that there is also a small peak in $T_{TbTb}(r)$ around 4 Å, with $R_{TbTb} < 2R_{TbO}$, due to a small amount of shared O_{nb} (8%).

Experimental data on RE–RE correlations is very difficult to obtain. The first such result was reported by Salmon and co-workers for glasses with RE = Dy/Ho and $x = 0.22$ (using isomorphic substitution) [12]. The experimental $T_{RE-RE}(r)$ reported by Salmon and co-workers does not show the presence of short RE–RE distances clearly. A peak at 4.72 Å was reported, but this was not conclusively identified as a real feature. However, they do report a value of 19% of O_{nb} neighbours to be shared, and this must involve some short RE–O_{nb}–RE distances. Results have also been reported by Newport and co-workers for glass with RE = Tb and $x = 0.26$ (using magnetic neutron scattering) [26]. Figure 6(a) shows the experimental Tb–Tb partial structure factor $S_{TbTb}(Q)$ [26], and the model results are in promising agreement. (The model results were calculated from the $T_{TbTb}(r)$ by Fourier transform, according to equation (4).) Note that the experimental $S_{TbTb}(Q)$ has units of barns steradians^{-1} atoms^{-1}

(left-hand y-axis), and hence is proportional to the model $S_{\mathrm{TbTb}}(Q)$ (right-hand y-axis). In addition, the experimental signal becomes negligible by $Q \sim 7$ Å^{-1} due to the magnetic form factor for Tb^{3+} [26]. Also shown in figure 6(a) as a dotted line is the $S_{\mathrm{TbTb}}(Q)$ calculated from the model after removing the small peak around 4 Å in $T_{\mathrm{TbTb}}(r)$. Although this has a noticeable affect on $S_{\mathrm{TbTb}}(Q)$, it is not clear whether the uncertainty in experimental results is low enough to distinguish the presence or absence of some short Tb–Tb distances. Figure 6(b) shows experimental $S_{\mathrm{RE-RE}}(Q)$ values reported in [12] for glasses with $x \approx 0.22$ and RE = Dy/Ho, and the two main peaks at $Q \sim 1.5$ and 2.5 Å^{-1} are similar to those in figure 6(a).

The model of Tb metaphosphate glass has some Q^1 and Q^3 units, and also has some O_{nb} with zero or two bonds to Tb, and these are not consistent with a more ordered conceptual model in which there are 100% Q^2 units, and 100% of O_{nb} bonded to one Tb. On average, each O_{nb} belonging to Q^1, Q^2 and Q^3 units has a bond valence of 1.33, 1.5 and 2.0 (respectively) for bonds to P, and so has an available bond valence of 0.67, 0.5 and 0.0 (respectively) for bonds to Tb. Hence an O_{nb} with zero bonds to Tb (i.e. a bond valence of 0.0 for bonds to Tb) will be well matched to Q^3 units, and not well matched to Q^1 units. On this basis, it is expected that O_{nb} with zero bonds to Tb is more likely to be found on Q^3 units, and less likely to be found on Q^1 units. Conversely, O_{nb} with two bonds Tb (i.e. shared O_{nb}) can be expected to have bond valence for bonds to Tb of ∼1.0 (assuming a typical bond valence of ∼0.5 for Tb–O bonds). The mismatch in bond valence will be smaller if such an O_{nb} belong to Q^1 units (a mismatch in bond valence of 1.0 versus 0.67) than if such an O_{nb} belong to Q^3 units (a mismatch in bond valence of 1.0 versus 0.0). On this basis, such an O_{nb} is most likely to be found on Q^1 units, and unlikely to be found on Q^3 units. Inspection of the model confirms these predictions. RE metaphosphate crystals have 100% Q^2 and 100% of O_{nb} with (at least) one bond to Tb, in accordance with the more ordered conceptual model discussed above. However, RE metaphsophate crystals have very anisotropic structures, with columns of RE ions and infinite spiral chains of Q^2 units aligned along the c-axes. In contrast, the glass must have an isotropic structure (and this is consistent with the presence of some finite rings in the model). One possible explanation for the presence of some Q^1 and Q^3 units, and a few O^{nb} with zero or two bonds to Tb, is that they enable an isotropic structure of the phosphate network in the glass. Alternative explanations are that these features of the model arise due to the very high quench rates in MD modelling, or due to limitations in the accuracy of the potential that is used.

5. Conclusion

The current study reports the first MD model of an RE phosphate glass, in this case Tb metaphosphate glass. The model is in good agreement with experimental results for nearest-neighbour distances and coordination numbers, and in reasonable agreement for x-ray and neutron diffraction structure factors. There is a tetrahedral phosphate network, with marked splitting of P–O_b and P–O_{nb} distances, which is a characteristic of phosphate glasses. The phosphate network has an average connectivity of $n = 2.1$ with mostly Q^2 groups, as expected for the metaphosphate composition, but with some Q^1 and Q^3 groups. Most Tb have a coordination of 6, and the average coordination is $N_{\mathrm{TbO}} = 5.7$, which compares favourably with experimental results that indicate $N_{\mathrm{RE-O}} \sim 6$ in metaphosphate glasses with small RE ions. The great majority of O_{nb} are bonded to only one Tb, but there are a few O_{nb} bonded to zero or two Tb, the latter occurring in Tb–O_{nb}–Tb configurations. These cause a small peak in Tb–Tb correlations around 4 Å, prior to the main peak around 6 Å. The corresponding Tb–Tb partial structure factor is in promising agreement with a recent experimental measurement using magnetic neutron scattering. One possible explanation for the presence of some Q^1 and

Q^3 groups, and of a few O_{nb} with zero or two bonds to Tb, is that they enable an isotropic structure of the phosphate network in the glass.

Acknowledgments

We are grateful for funding from the UK Engineering and Physical Sciences Research Council (EPSRC), and to Newport and co-workers for access to data prior to publication.

References

[1] Shelby J E 2005 *Introduction to Glass Science and Technology* (Cambridge: RSC) p 60
[2] Weber M J 1991 *Materials Science and Technology* vol 9, ed J Zrzycki (Weinheim: VCH) p 654
[3] Hoppe U, Kranold R, Stachel D, Barz A and Hannon A C 2000 *Z. Naturf.* a **55** 369
[4] Mierzejewski A, Saunders G A, Sidek H A A and Bridge B 1988 *J. Non-Cryst. Solids* **104** 323
[5] Ilieva D, Jivov B, Kovacheva D, Tsacheva T, Dimitriev Y, Bogachev G and Petkov C 2001 *J. Non-Cryst. Solids* **293–295** 562
[6] Meyer K 1997 *J. Non-Cryst. Solids* **209** 227
[7] Rashid N E, Phillips B L and Risbud S H 2000 *J. Mater. Res.* **15** 2463
[8] Cole J M, van Eck E R H, Mountjoy G, Anderson R, Brennan R, Bushnell-Wye G, Newport R J and Saunders G A 2001 *J. Phys.: Condens. Matter* **13** 4205
[9] Cole J M, van Eck E R H, Mountjoy G, Newport R J, Brennan T and Saunders G A 1999 *J. Phys.: Condens. Matter* **11** 9165
[10] Hoppe U, Metwalli E, Brow R K and Neuefeind J 2002 *J. Non-Cryst. Solids* **297** 263
[11] Martin R A, Salmon P S, Benmore C J, Fischer H E and Cuello G J 2003 *Phys. Rev.* B **68** 054203
[12] Martin R A, Salmon P S, Fischer H E and Cuello G J 2003 *Phys. Rev. Lett.* **90** 185501
Martin R A, Salmon P S, Fischer H E and Cuello G J 2003 *J. Phys.: Condens. Matter* **15** 8235
[13] Anderson R, Brennan T, Cole J M, Mountjoy G, Pickup D M, Newport R J and Saunders G A 1999 *J. Mater. Res.* **14** 4706
[14] Cole J M, Newport R J, Bowron D T, Pettifor R F, Mountjoy G, Brennan T and Saunders G A 2001 *J. Phys.: Condens. Matter* **13** 6659
[15] Hoppe U, Kranold R, Stachel D, Barz A and Hannon A C 1998 *J. Non-Cryst. Solids* **232–234** 44
[16] Hoppe U, Ebendorff-Heidepriem E, Neuefeind J and Bowron D T 2001 *Z. Naturf.* a **56** 1
[17] Hoppe U, Brow R K, Ilieva D, Jovari P and Hannon A C 2005 *J. Non-Cryst. Solids* **351** 3179
[18] Karabulut M, Marasinghe G M, Metawalli E, Wittenauer A K, Brow R K, Booth C H and Shuh D K 2002 *Phys. Rev.* B **65** 104206
[19] Hong H Y P 1974 *Acta Crystallogr.* B **30** 468
[20] Hong H Y P 1974 *Acta Crystallogr.* B **30** 1857
[21] Hoppe U 1996 *J. Non-Cryst. Solids* **195** 138
[22] Liang J J, Cygan R T and Alam T M 2000 *J. Non-Cryst. Solids* **263/264** 167
[23] Speghini A, Sourial E, Peres T, Pinna G, Bettinelli M and Capobianco J A 1999 *Phys. Chem. Chem. Phys.* **1** 173
[24] Sourial E, Peres T, Capobianco J A, Speghini A and Bettinelli M 1999 *Phys. Chem. Chem. Phys.* **1** 2013
[25] Mountjoy G, Anderson R, Bowron D T and Newport R J 1998 *J. Non-Cryst. Solids* **232–234** 227
[26] Cole J M, Hannon A C, Martin R A and Newport R J 2006 *Phys. Rev.* B **73** 104210
[27] Teter D 2004 private communication
[28] Cormack A N and Du J 2004 *J. Non-Cryst. Solids* **349** 66
[29] Thomas B W M, Mead R N and Mountjoy G 2006 *J. Phys.: Condens. Matter* **18** 1
[30] Gale J D 1997 *JCS Faraday Trans.* **93** 629 (Version 1.2. 2002)
[31] Fletcher D A, McMeeking R F and Parkin D 1996 *J. Chem. Inf. Comput. Sci.* **36** 746 (The United Kingdom Chemical Database Service)
[32] Smith W, Forester T R, Greaves G N, Haytera S and Gillan M J 1997 *J. Mater. Chem.* **7** 331
[33] Smith W and Forester T 1996 *J. Mol. Graphics* **14** 136
[34] Corrales L R and Du J 2005 *Phys. Chem. Glasses* **46** 420
[35] Du J and Cormack A N 2001 *J. Non-Cryst. Solids* **293–295** 283
[36] Mead R N and Mountjoy G 2005 *Phys. Chem. Glasses* **46** 311
[37] Elliott S R 1990 *Physics of Amorphous Materials* (Harlow: Longman) p 91
[38] Hoppe U 2000 *J. Phys.: Condens. Matter* **12** 8809